Journal of Alloys and Compounds 509 (2011) 6009–6014

Contents lists available at ScienceDirect

Journal of Alloys and Compounds

journal homepage: www.elsevier.com/locate/jallcom

Charge growth, dispersion in europium manganite ($EuMnO_{3-\delta}$) ceramics revealed using opto-impedance probe

S. Radhakrishnan, R. Jagannathan*

Central Electrochemical Research Institute, Karaikudi-630006, T.N., India

ARTICLE INFO

Article history:
Received 6 October 2010
Received in revised form 14 February 2011
Accepted 16 February 2011
Available online 11 March 2011

Keywords:
Ceramics
Magnetic materials
Electronic-structure
Optical properties
Impedance

ABSTRACT

In this preliminary report, we present the impedance characteristics of poly-crystalline europium manganite, a promising colossal magneto resistance (CMR) system investigated under optical (~5 eV) and magnetic (0.1 T) perturbations yielding some clues on the charge build-up and dispersion processes. This may possibly be resulting from switching between ferromagnetic and anti-ferromagnetic phases through a charge transfer transition mediated process centering $Mn^{3+/4+}$ 3d spins thereby meriting a more detailed study correlating with magnetic measurements.

1. Introduction

Giant magneto resistance effect facilitating better data storage has revolutionized the digital world. In the same way the advent of colossal magneto resistance (CMR) effect based on pervoskite type lanthanide manganites is poised for significant enhancement in data storage density eventually paving way for still greater leaps in digital computing, provided temperature of the effect can be raised suitably. Hence rare-earths/lanthanide manganites (Ln = La, Eu, Gd, Dy, Tb) exhibiting exotic CMR properties constitute an important system of materials both from fundamental and application standpoints [1,2].

There is sustained increase in multi-faceted investigations on various manganites covering academic and application interests, in particular spin-density, switching behavior, configuration, colossal thermoelectric power, interesting tunneling microscopy properties and so on [3–7]. Although the spin-structure of Mn-sites determines the ferro-electric ordering in this system of materials, the presence of lanthanide ions can also significantly modulate this ordering and hence mulitferroic properties [8]. Of all the lanthanide manganites, the $EuMnO_3$ system may be different because this system exhibits some anomaly in anti-ferromagnetic ordering with respect to temperature [9]. Fortuitously the Eu^{3+} ion can exhibit intense photo-induced metal to ligand (Eu^{3+}-O^{2-}) $4f^7 2p^{-1}$ charge transfer transition in the energy region of ~5 eV under optical pumping. Hence it is thought worthwhile to employ the opto-impedance method [10,11] in conjunction with application of magnetic field.

It is pertinent to note that there is already a report on change in photoconductivity of these manganites upon illumination using UV or visible radiation [12].

2. Experimental details

Phase-singular polycrystalline $EuMnO_3$ ceramic sample was synthesized through a conventional multi-stage solid-state reaction in air-atmosphere with intermittent homogenization steps. Because the synthesis conditions of the present sample is different from that of the standard sample there may be some change sample conditions, in particular the oxygen stoichiometry. Chemical phase purity of the sample synthesized was ascertained in terms of X-ray powder diffraction pattern consistent with standard JCPDS files # 26-1126 corresponding to the $EuMnO_3$ phase (Fig. 1). In this figure, the low intensity (~10%) of the XRD diffraction lines beyond $2\theta \geq 45^\circ$ causes some difficulty in clear matching with the JCPDS file. We can observe a small shift in XRD lines towards to higher 2θ values with respect to the positions corresponding the JCPDS file indicating a marginal decrease in interplanar *d*-spacing. The obtained XRD data were refined using a standard least squares refinement procedure and the refined crystallographic cell parameters thus obtained were consistent with standard values as given in Table 1, thereby confirming the chemical identity and integrity of the sample investigated. The oxygen content of the $EuMnO_3$ sample studied, must be having very crucial role in determining the magnetic, CMR properties. But in this preliminary report we could not make any measurements on the oxygen content in the ceramics. For this reason we prefer to indicate the sample studied using the formula $EuMnO_{3-\delta}$ with the $\pm\delta$ being the deviation from stoichiometry in the oxygen content of the investigated sample.

For opto-impedance measurements, the experimental conditions were the same as described before [11,13]. For opto-impedance measurements we used a 15 W short-wave UV lamp with 90% of radiation concentrated at λ_{max} = 254 nm. The ceramics sample used in this study was in circular disc form with dimensions, 20 mm

* Corresponding author. Tel.: +91 9487167780; fax: +91 4565 227713.
E-mail address: jags57_99@yahoo.com (R. Jagannathan).

0925-8388/$ – see front matter © 2011 Elsevier B.V. All rights reserved.
doi:10.1016/j.jallcom.2011.02.081

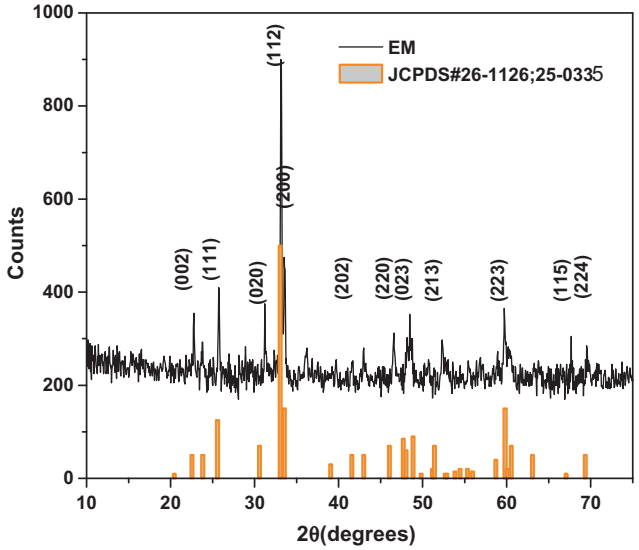

Fig. 1. XRD pattern of $EuMnO_3$ ceramics synthesized.

(diameter), 2 mm (thickness) and the UV penetration depth in the sample is expected to be in the range of 15–20 μm.

For magneto-impedance measurements, we used a cylindrical magnet of field strength 0.1 ± 0.005 T. Owing to experimental limitations we could carry-out magneto-impedance measurements only at this field and in future we plan to extend the study to low and high field ranges. In this report for reasons of brevity we present impedance patterns of some representative examples of raw data and fitted data for all samples/conditions.

3. Results and discussion

The solid state impedance profiles of polycrystalline $EuMnO_3$ ceramics measured under different conditions are compiled in Figs. 2–4. At room temperature, the solid state impedance profile [complex plane impedance plot (CPIP) also referred as Nyquist plot)] of the $EuMnO_3$ ceramics exhibits a semi-circular loop indicating the presence of a classical Voigt element exhibiting some dispersion in the low frequency side accompanied by a spiral like tail attached in the high frequency end ~50 kHz indicated by an arrow (Fig. 2a). These features do not seem to undergo any spectacular change at room temperature even under optical pumping of UV photons. However upon application of magnetic field the spiral like tail in the high frequency end undergoes some deformation resembling overlapped linear patterns at the high frequency end as indicated by an arrow (Fig. 2b).

On the other hand, when the sample is cooled down to liquid nitrogen temperature (LNT), the impedance features change drastically. At LNT, the impedance profile reduces to a linear profile running nearly parallel to the *y*-axis indicating the presence of only imaginary part of the capacitive impedance (Fig. 3c). While upon optical/UV pumping, this linear impedance profile undergoes a dispersion like feature wherein we observe a dispersed line accompanied by a semi-circular profile suggesting the re-emergence of the voigt element (Fig. 3d) as well. Furthermore the application of magnetic field results in the loss of spiral like feature in the high

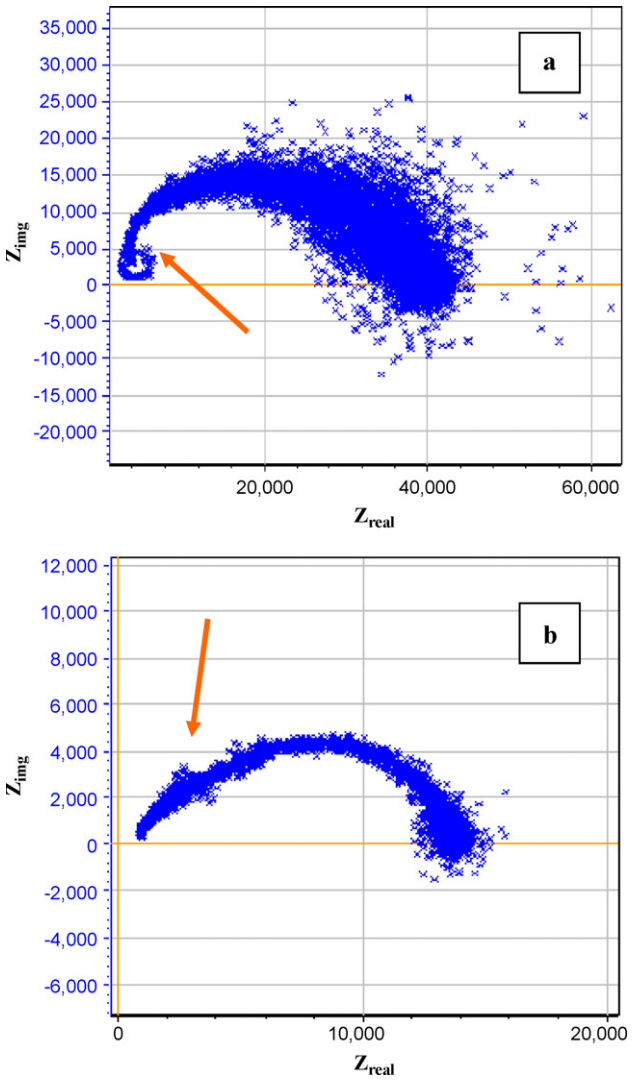

Fig. 2. Complex plane impedance plot of $EuMnO_3$ synthesized. (a) Under normal condition at RT (room temperature). (b) Under magnetic perturbation at RT (room temperature).

frequency end (Fig. 4a and b). When cooled down to LNT, we can see that the application of magnetic field makes the linear profile to show an angle (Fig. 4c) indicating the presence of a resistive component along with some capacitive impedance. Also it should be noted that along with application of magnetic field, exposure of the sample to UV radiation leads to a magneto opto-impedance spectrum. The impedance spectrum thus obtained shows a more diffused semicircle accompanied by a strong inductive loop in the high frequency region ~50–100 kHz (Fig. 4d).

In the complex-plane impedance Nyquist plot a semicircular impedance profile can be explained using an effective impedance

$$Z = \frac{R}{1+\omega^2R^2C^2} - \frac{J\omega R^2C}{1+\omega^2R^2C^2} \quad (1)$$

Table 1
Least squares refined crystallographic unit-cell parameters for EuMnCb sample (space group-*Pbnm*).

System	Refined cell parameters (Å)			Standard deviation (σ)
	a	*b*	*c*	
JCPDS standard -#26-1126 also 25-0335	5.336	5.842	7.451	a_a = +0.004 a_b = +0.009
$EuMnO_3$ – as synthesized	5.332	5.833	7.461	a_c = ±0.010

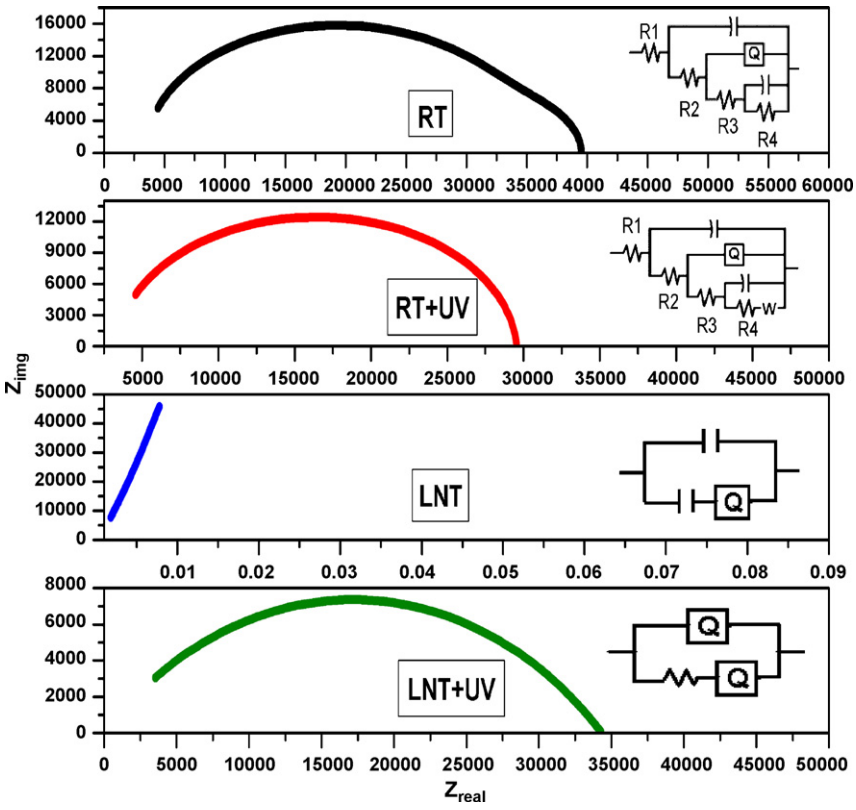

Fig. 3. Complex plane impedance plot of $EuMnO_3$ ceramics with and without UV (optical-perturbation), at room temperature (RT) and at liquid nitrogen temperature (LNT).

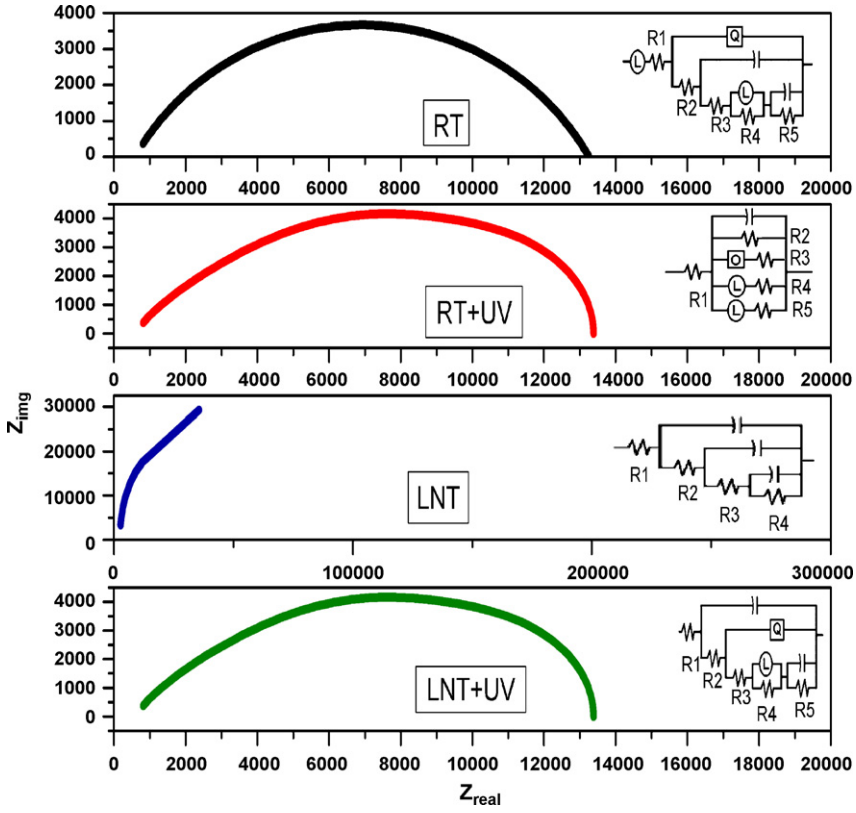

Fig. 4. Complex plane impedance plot of $EuMnO_3$ ceramics with and without UV (optical, magnetic perturbation), at room temperature (RT) and at liquid nitrogen temperature (LNT).

Table 2
Fitted parameters on opto-impedance characteristics of $EuMnO_3$.

Temperature and conditions	Impedance components C in farad R in ohms	Phase element (Φ)	Remarks
RT	$C_1 = 2.7 \times 10^{-11}$, $R_2 = 3.13 \times 10$ (V) $C_2 = 2.1 \times 10^{-9}$, $R_4 = 4.4 \times 10^5$ (V) $R_1 = 3.453$, $R_3 = 348.7$ (S)	1.2×10^{-6} (0.329)	Semi circular loop indicating voigt element.
RT + UV	$C_1 = 3.01 \times 10^{-11}$, $R_2 = 2.3 \times 10$ (V) $C_2 = 4.3 \times 10^{-1}$, $R_4 = 0.01$ (V) $R_1 = 3361$, $R_3 = 2656$ (S)	2.4×10^{-9} (1)	Semi circular loop Indicating voigt element
LNT	$C_1 = 1.5 \times 10^{-11}$ $C_2 = 1.1 \times 10^{-6}$	2.34×10^{-6} (0.8)	Charge build up suggesting capacitive impedance
LNT + UV	$R = 4408$	2.9×10^{-5} (0.8) 1.9×10^{-9} (0.8)	Collapse of charge ordering, reemergence of voigt element.

V: voigt element; S: series element.

with ω, R, C, respectively being the angular frequency, ohmic resistance and capacitance of the ceramic sample as the dielectric across the silver contacts. But in actual measurement conditions, the situation turns out to be a more complex because of the presence of various impedance components *viz*., grain-interior, grain-boundary and contact electrode interfaces.

The opto-impedance and also the magneto opto-impedance studies of this ceramic system are expected to be limited by the skin–effect from the fact that $\omega_{optical} \sim 10^{15}$ Hz $\gg \omega_{applied} \sim 10^6$ Hz reflected in the probe-depth δ given by

$$\delta = \sqrt{\frac{2\rho}{\omega\mu}} \quad (2)$$

with ρ, ω, μ, respectively being the resistivity of the ceramics, angular frequency of the applied/perturbation; μ-magnetic permeability of the ceramic system. However this limitation can be mitigated from the fact that the $EuMnO_3$ ceramic system is of high resistivity.

On careful comparison of the opto-impedance and magneto opto-impedance spectra at room temperature it can be concluded that the difference is not very substantial in terms of patterns and magnitudes. The observation that at room temperature the Voigt geometry remains intact even under optical, magneto-optical perturbations confirms this conclusion (Figs. 3a, b and 4a, b). On other hand the situation turns out to be more interesting as the ceramic sample is cooled down to LNT. The linear profile running nearly parallel to the ordinate of the two-dimensional complex plane impedance plot indicates a kind of charge build-up (Fig. 3c). In the CPIP, the occurrence of a sloping line indicates an anomalous dispersion behavior of capacitance [14]. More significant observation is that there is significant increase in the capacitance in the high-frequency region (50–550 kHz) indicating a mammoth charge build-up which may be in the bulk of the ceramics (Table 2). Furthermore upon application of magnetic field the temporal-span for this charge build-up process is further shortened (200–900 kHz) (Fig. 4c).

The collapse of Voigt element followed by the emergence of a capacitor element along with constant phase element(s) may lead to some interesting conclusions. At LNT the collapse of Voigt element and the sudden surging of charges suggesting mammoth charge buildup in capacitance value indicates the presence of just capacitor component alone. This clearly suggests a dominant charge growth process in this system. Simultaneously for the resistive component (R) it should be mentioned that either it is absent or there is considerable decrease in resistivity which can be attributed to an entirely different process *viz*., the CMR property leading to enhanced conductivity at low temperatures.

Upon UV shining this charge build-up process seems to be disturbed and the profile branches into two components *viz*., a vertical component indicating a CPE in the high frequency region (∼50–100 kHz) and a Voigt element in the low frequency region (<50 kHz). Of these two components the vertical component with constant phase-element does not encounter any resistive part while the latter encounters a significant resistance of the same order as does at $T = 300$ K. In all fairness, this condition seems to suggest a more conducting phase like a metallic conductor for the former while an insulating phase for the latter. This is in line with reports on emergence of two phases *viz*., showing ferro-magnetic and anti-ferromagnetic ordering in several pervoskite-manganites upon doping [15,16]. These two processes seem to compete with each other and determined by various factors like temperature, dopants [17,18]. It is important to note that at LNT, the magnitude of impedance, also the constant phase element (Φ) of

Table 3
Fitted parameters on magneto opto-impedance characteristics of $EuMnO_3$.

Temp and condition	Impedance components (LCR) C in farad R in ohms L in henry	L Henry	Phase element (Φ)	Remarks
RT + magnet	$C_1 = 6.4 \times 10^{-9}$, $R_3 = 2538$ (V) $C_2 = 1.7 \times 10^{-4}$, $R_5 = 0.174$ (V) $R_1 = 610$, $R_2 = 1 \times 10^4$ (S)	1×10^{-15}	5.6×10^{-8} (0.675)	Semi circular loop indicating voigt element, at the high frequency end some inductive loop superimposed.
RT + magnet + UV	$C_1 = 1.9 \times 10^{-10}$, $R_2 = 3.4 \times 10^4$ (V) $R_1 = 648$ (S)	9.8×10^{-3}	5.5×10^{-7} (0.02)	Semi circular loop indicating voigt element, at the high frequency end some inductive loop superimposed.
LNT + magnet	$C_1 = 1.6 \times 10^{-11}$, $R_2 = 5.1 \times 10^5$ (V) $C_2 = 2.6 \times 10^{-12}$, $R_3 = 1824$ (V) $C_3 = 1.3 \times 10^{-8}$, $R_4 = 5.2 \times 10^2$ (V) $R_1 = 2791$ (S)	-	-	Charge build-up along y-axis, inductive loop vanishes.
LNT + magnet + UV	$C_1 = 4.73 \times 10^{-11}$, $R_2 = 915.9$, $C_2 = 2.3 \times 10^{-10}$, $R_5 = 1213$ (V) $R_1 = 0.01$, $R_3 = 4.35$ (S)	0.02	3.26×10^{-8} (0.73)	Re-emergence of voigt element with inductive loop.

V: voigt element; S: series element.

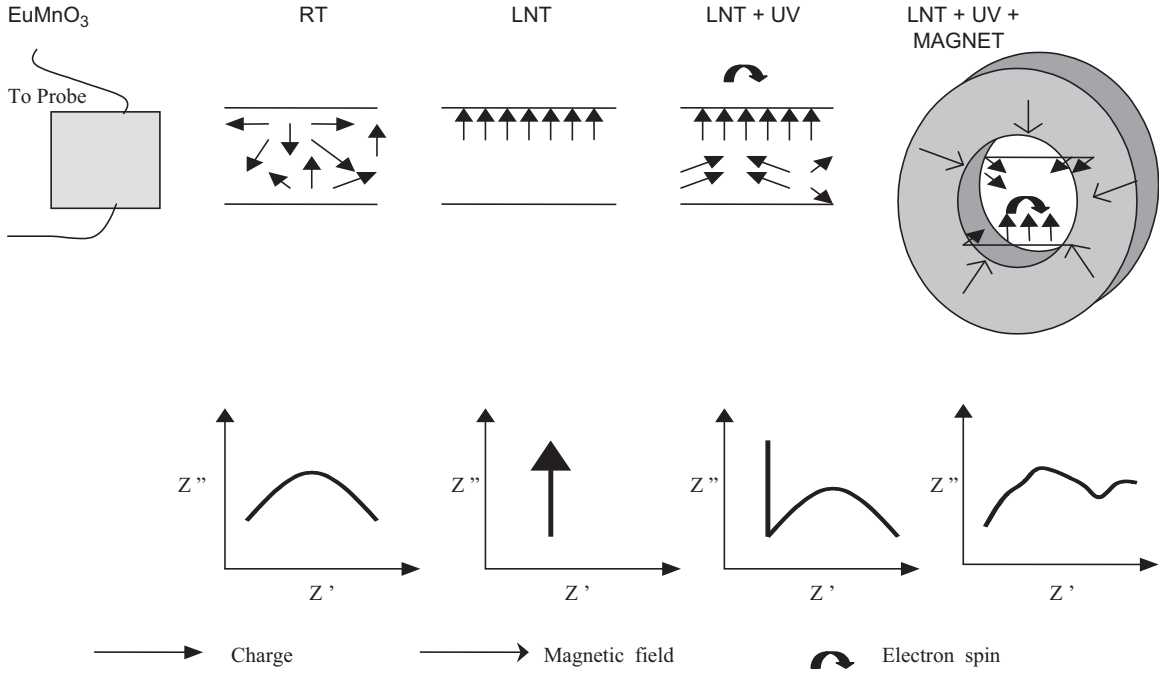

Fig. 5. Schematics illustrating impedance measurement configuration and the profiles.

the linear component are same in both cases of dark and UV shining.

It turns out that for the magneto opto-impedance results, the CPIP acquires a more complex picture. The spiral like pattern observed at room temperature indicating an apparent inductive loop feature in the high frequency region undergoes a significant modification upon magnetic perturbation. The application of magnetic field is expected to perturb the spin structure of the manganese ion(s) rather than europium ion(s). The 4*f* magnetic moment due to Eu^{3+} center(s) may get quenched at low temperatures [19]. Also these rare-earth manganites exhibit modulated spin structures eventually determining their polarization and dielectric properties arising from frustrated exchange interactions having profound dependence on ionic size of the lanthanide ions [8,20,21]. $EuMnO_3$ system having an acentric *Pbnm* orthorhombic lattice symmetry exhibits giant magneto-capacitance effect attributed to frustration in sinusoidal antiferromagnetic ordering at low temperatures, in particular thermally induced anomalous behavior of dielectric constant component ε_c of this manganite system [8]. On the otherhand, in the Mn-sites, the $Mn^{3+/4+} \leftrightarrow O^{2-}(2p^{-1})$ metal to ligand type charge transfer transition lies in the UV region ($\sim$37,000 cm^{-1}) in several manganese oxide matrices [22,23] being very close to the energy of the optical perturbation. This charge transfer transition being $d \leftrightarrow p$ Laporte allowed is very intense and can efficiently facilitate the charge transfer transition there by accomplishing Mn^{3+} to Mn^{4+} and back charge transfer transitions through metal to ligand and ligand to metal charge transfer transitions respectively with the latter transition being energetically more favorable [24]. The UV perturbation might lead to optical-excitation and subsequent relaxation of Mn-centers leading to photo-oxidation–reduction processes resulting in the formation of a redox couple centering Mn-sites eventually leading to flip-fop in the Mn-valence states between 3+ and 4+ states.

It has been reported that the Neel temperature (T_N) of the system under investigation is known to be around $\sim$50 K [25]. Hence it seems reasonable to expect that the results of the present investigation at LNT being closer to T_N might give some clues on switching of magnetic ordering between anti-ferromagnetic to paramagnetic phases. It is pertinent to note that the off-stoichiometry in $EuMnO_3$ composition either in europium content or oxygen vacancies/defects can significantly influence the magnetic, also the CMR properties [26]. Furthermore it is reasonable to expect that the UV perturbation in the energy region corresponding to Eu-oxygen, Mn-oxygen charge transfer transition regions may act as a switch between ferromagnetic and anti-ferromagnetic phases. At this time owing to experimental limitation we could not carry out any such magnetic measurements.

From Table 3 we have that the presence or absence of inductive component (L) and its value are very much dependent on the kind of perturbation the sample is subjected to. The whole process of opto-impedance, magneto opto-impedance can be pictorially schematized as given in Fig. 5. At LNT, the accumulation of charges leading to pronounced enhancement in capacitance based impedance in a particular the region is illustrated by collection of aligned arrows in one electrode which upon optical (UV) pumping partly gets dispersed while this process gets more compounded upon magnetic perturbation interacting with electron-spin(s). This condition may lead to an inductive impedance.

4. Conclusions

In conclusion we believe that this preliminary report may open up some new possibilities for investigating the charge ordering-dispersion property of this technologically important manganite system meriting extensive studies. Further insights on magnetic ordering property of this system may be possible using vibration magnetometer studies which is planned for our future work.

Acknowledgments

Our sincere thanks to Dept of Science & Technology, New Delhi and CECRI, Karaikudi-CSIR, New Delhi for the project grant and the support we received. Also it is pleasure to express our sincere thanks to the editor, referees for their valuable suggestions in improving the manuscript.

References

[1] N.A. Spaldin, M. Fiebig, Science 309 (2005) 391–392.
[2] Y. Ding, D. Haskei, Y. Tseng, E. Kaneshita, M.V. Veenendal, J.F. Mitchell, S.V. Sinogeikin, V. Prakapenka, H.K. Mao, Phys. Rev. Lett. 102 (2009) 237201.
[3] B. Fisher, J. Genossar, L. Patlagan, S. Kar-Narayan, X. Moya, J.C. Loudon, N.D. Mathur, Nat. Mater. 9 (2010) 688–690.
[4] S. Sagar, V. Ganesan, P.A. Joy, Senoy Thomas, A. Liebig, M. Albrecht, M.R. Anantharaman, Eur. Phys. Lett. 91 (2010), 17008.
[5] J. Salafranca, S. Okamoto, Phys. Rev. Lett. 105 (2010) 256804–256807.
[6] S. Yu Prilipko, G.Ya. Akimov, Yu.F. Revenko, V.N. Varyukhin, A.A. Novokhatskaya, Low Temp. Phys. 36 (2010) 357–359.
[7] I. Mazzaccari, H. Jeen, A. Biswas, Bull. Am. Phys. Soc. Abstract B0.00009 (March 2011).
[8] T. Goto, T. Kimura, G. Lawes, A.P. Ramirez, Y. Tokura, Phys. Rev. Lett. 92 (2004) 257201–257204.
[9] W.S. Ferreria, J.A. Moreira, A. Almeida, J.P. Araujo, P.B. Tavares, T.M. Mendonca, P.S. Carvalho, S. Mendonca, Ferrorelectrics 368 (2008) 107.
[10] P. Kalyani, S. Sivasubramanian, S. Naveen Prabhu, K. Ragavendran, N. Kalaiselvi, N.G. Ranganathan, S. Madhu, A. Sundara Raj, S.P. Manoharan, R. Jagannathan, J. Phys. D: Appl. Phys. 38 (2005) 990–996.
[11] A. Nakkiran,,J. Thirumalai, R. Jagannathan, Chem. Phys. Lett. 436 (2007) 155–161.
[12] A. Gilabert, R. Cauro, M.G. Medici, J.C. Grenet, H.S. Wang, Y.F. Hu, Qi. Li, J. Supercond. 13 (2000) 285–290.
[13] K. Ragavendran, A. Nakkiran, P. Kalyani, A. Veluchamy, R. Jagannathan, Chem. Phys. Lett. 456 (2008) 110–115.
[14] E. Barsoukov, J. Ross Macdonald (Eds.), Impedance Spectroscopy: Theory, Experiment, and Applications, second ed., John Wiley & Sons, Inc., New York, 2005, p. 494.
[15] H. Qin, J. Hu, J. Chen, Y. Wang, Z. Wang, J. Appl. Phys. 91 (2002) 10003.
[16] N. Volkov, G. Petrakovskii, P. Boni, E. Clementyev, K. Patrin, K. Sablina, D. Velikanov, A. Vasiliev, J. Magn. Magn. Mater. 309 (2007) 1–6.
[17] A. Maignan, C. Martin, G. Van Tendeloo, M. Hervieu, B. Raveau, Phys. Rev. B 60 (1999) 15214–15219.
[18] E. Dagotto, J. Burgy, A. Moreo, Solid State Commun. 126 (2003) 9–22.
[19] K. Noda, M. Akaki, T. Kikuchi, D. Akahoshi, H. Kuwahara, J. Appl. Phys. 99 (2006), 08S905-1-8S905-3.
[20] A.M. Kadomtseva, Yu.F. Popov, G.P. Vorobev, V.Yu. Ivanov, A.M. Mukhin, A.M. Balbashov, JETP Lett. 81 (2005) 590–593.
[21] T. Kimura, T. Goto, H. Shintani, K. Ishizaka, T. Arima, Y. Tokura, Nature 426 (2003) 55–58.
[22] D.M. Sherman, Am. Miner. 69 (1984) 788–790.
[23] K. Langer, R.M. Abu-Eid, Phys. Chem. Miner. 1 (1977) 273–276.
[24] C. Zener, Phys. Rev. 82 (1951) 403–405.
[25] A.A. Mukhin, V.Yu. Ivanov, V.D. Travkin, V.A.S. Prokhorov, A.M. Balbashov, J. Hemberger, A. Loidl, J. Magn. Magn. Mater. 272–276 (2004) 96–97.
[26] H.L. Ju, J. Gopalakrishnan, J.L. Peng, Q. Li, X. Xiong, T. Venkatesan, R.L. Greene, Phys. Rev. B 51 (1995) 6143–6147.